J. Phys. B: At. Mol. Opt. Phys. **23** (1990) 4625–4639. Printed in the UK

Electronic excitation of molecular hydrogen using the R-matrix method

Susan E Branchett†, Jonathan Tennyson† and Lesley A Morgan‡
† Department of Physics and Astronomy, University College London, London WC1E 6BT, UK
‡ Computer Centre, Royal Holloway and Bedford New College, Egham, Surrey TW20 0EX, UK

Received 20 August 1990

Abstract. Calculations are presented for electron–H_2 collisions for energies up to 25 eV. Excitation from the ground, X $^1\Sigma_g^+$, to the lowest six excited electronic states, b $^3\Sigma_u^+$, a $^3\Sigma_g^+$, c $^3\Pi_u$, B $^1\Sigma_u^+$, E,F $^1\Sigma_g^+$ and C $^1\Pi_u$, is explicitly considered for all total symmetries up to and including $^2\Phi_g$. The target states are represented using a full configuration interaction treatment within a basis of Slater-type orbitals optimized to give accurate vertical excitation energies. Results are presented for eigenphase sums, in which the resonant and other features are analysed, as well as total electronic excitation cross sections. Extensive comparison is made with the available experimental data. In contrast to many previous *ab initio* calculations our results are in good agreement with the observed electronic excitation cross sections for all the processes considered.

1. Introduction

One of the most fundamental processes in molecular physics is the collision of electrons with molecular hydrogen, a process which is important for both astrophysics (Shemansky *et al* 1985) and in plasmas (Tawara and Phaneuf 1988). However, even for this seemingly simple process there are many gaps in our knowledge (McConkey *et al* 1988).

Experimentally there have been several studies of the series of resonances observed in the 10–15 eV region. The early work on this problem was comprehensively reviewed by Schulz (1973); more recent studies include those of Spence (1974), Weingartshofer *et al* (1975), Bose and Linder (1979) and Mason and Newell (1986a). Altogether there is a considerable body of data on these resonance series but no consistent pattern of explanation.

Much of the more recent experimental effort has concentrated on measuring non-resonant differential and total cross sections for the various electronic excitation processes (Watson and Anderson 1977, Ajello *et al* 1982, 1984, Hall and Andric 1984, Pasquerault *et al* 1985, Mason and Newell 1986b, Khakoo and Trajmar 1986, Nishimura and Danjo 1986, Khakoo *et al* 1987). These measurements are difficult and, in particular, it is often not possible to obtain reliable total cross sections; exactly the data required when modelling astrophysical or plasma processes. A compilation of these data has recently been published by Tawara *et al* (1990).

Theoretically the situation is also far from satisfactory. Although there have been some calculations of resonance parameters using Feshbach or stabilization methods (Elizer *et al* 1967, Buckley and Bottcher 1977, Bardsley and Cohen 1978, DeRosa *et al* 1988), there has been little recent work on the 10–15 eV resonance problem, and, to our knowledge, only very limited attempts have been made to study these features using scattering methods (da Silva *et al* 1990). Conversely considerable recent effort has gone into calculating non-resonant differential and total cross sections (see for example Fliflet and McKoy 1980, Arrighini *et al* 1980, Lee *et al* 1982, Redmon *et al* 1985, Baluja *et al* 1985, Schneider and Collins 1985, Lima *et al* 1985, Gibson *et al* 1987, Rescigno and Schneider 1988, Lima *et al* 1988, Lee *et al* 1990).

Until very recently a common feature of all these calculations was the use of coupled-state expansions limited to the initial and final target states, and target states represented by single-configuration wavefunctions, often a poor approximation for excited states. Thus, for example, in a coordinated study Baluja *et al* (1985), Schneider and Collins (1985) and Lima *et al* (1985) computed the X $^1\Sigma_g^+ \rightarrow$ b $^3\Sigma_u^+$ excitation cross section using different procedures to solve for the same model (two coupled single-configuration target states). These calculations gave very similar results, but, as we shall show, the absence of multichannel or target polarization effects in the model considered meant that no resonance effects were observed near threshold and that the higher energy cross section was overestimated.

Very recently limited studies considering several coupled channels (da Silva *et al* 1990) and target correlation (Lee *et al* 1990) have appeared. It is clear that it is in this direction that any systematic improvement of the theory lies.

In this work we present the results of calculations which explicitly couple the lowest seven electronic states of H_2. Moreover, these states are represented by correlated wavefunctions which yield accurate thresholds for electronic excitation. This work thus represents a very significant improvement on previous theoretical attempts to treat this challenging problem. Branchett and Tennyson (1990), henceforth referred to as I, recently published preliminary results of these calculations. In I a six-state model was used to obtain resonance parameter in the 10–13 eV region. In this work the model is extended and detailed consideration is given to the electronic excitation cross sections involved.

2. Method

These calculations were performed using the molecular *R*-matrix method. This method, the theory of which has been presented in detail by Gillan *et al* (1987) and Morgan (1990), has been used successfully to study a number of elastic (e.g. Tennyson and Noble 1985, 1986, Gillan *et al* 1988, Tennyson 1988) and vibrationally inelastic (Morgan 1984b, Morgan and Burke 1988, Morgan *et al* 1990) electron collision processes as well as positron collisions (Tennyson 1986, Danby and Tennyson 1990). Early work using simple target representations for electronic excitation calculations (Tennyson *et al* 1984, Baluja *et al* 1985, Noble and Burke 1986) has recently been augmented by studies using correlated target functions (Branchett and Tennyson 1990, Gillan *et al* 1990).

In the *R*-matrix method space is divided into two regions. Inside the *R*-matrix sphere full electron–electron Coulomb and exchange interactions are considered; outside the sphere the target wavefunction is assumed to have negligible amplitude and the interactions can be expressed in terms of target multipoles (both diagonal and off-diagonal for a coupled-states calculation).

In this work we represent the H_2 target, with its internuclear separation fixed at 1.4 a_0, by the set of specially optimized Slater-type orbitals (STO) whose exponents are given in table 1. The STO were selected as follows. The three compact σ_g orbitals were taken from Fraga and Ransil (1961) who optimized them for the X $^1\Sigma_g^+$ ground state. The σ_u orbitals exponents were optimized for a SCF calculation on the lowest state of $^1\Sigma_u^+$ symmetry. The set of π_u orbitals was obtained by optimizing a SCF calculation on the lowest $^1\Pi_u$ state and the π_g orbitals were taken from Nesbet *et al* (1986). This basis gave a satisfactory representation of all the states of interest except the excited Σ_g^+ states. This problem was diagnosed as being due to the lack of diffuse σ_g orbitals and the diffuse ($\zeta = 0.600$) 2s(σ_g) orbital was added to the σ_g orbital set, its exponent being chosen by trial and error.

Table 1. Exponents of the Slater-type orbitals in the atomic orbital basis set used to represent the H_2 target.

Orbital	Exponent	Orbital	Exponent
1s(σ_g)	1.378	1s(σ_u)	1.081
2s(σ_g)	1.176	2s(σ_u)	0.800
2s(σ_g)	0.600		
2p(σ_g)	1.820	2p(σ_u)	1.820
2p(π_u)	0.574	2p(π_g)	1.084
3p(π_u)	0.636	3p(π_g)	1.084
3d(π_u)	1.511	3d(π_g)	2.470

The 6 state model used in I is augmented here by including the E,F $^1\Sigma_g^+$ state. This state lies close to, but below, the C $^1\Pi_u$ state included previously, and was shown to be important in the recent test calculations of da Silva *et al* (1990). Above the C $^1\Pi_u$ state there is a gap of 1.7 eV until the nearly degenerate i $^3\Pi_g$ and I $^1\Pi_g$ states (Kolos and Rychlewski 1977).

The wavefunction of each of the seven lowest states of H_2 was expressed as a full configuration interaction (CI) representation within the orbital basis described above. Table 2 gives the the number of configurations in each expansion and the resulting energies of each state. The energies of the excited states are given as (vertical) excitation energies relative to the ground state as it is the excitation thresholds which are important for scattering. For comparison we also give very accurate excitation energies from *ab initio* electronic structure calculations using large basis sets and, for attractive excited states, the observed $v = 0$ to $v = 0$ excitation energy. As can be seen, our excitation thresholds are a good approximation to the accurate energies, the worst being the B $^1\Sigma_u^+$ threshold which is 0.4 eV in error. In the calculations presented below we shifted the threshold, and associated diagonal Hamiltonian matrix elements, to correct for these small errors in the excitation thresholds.

Inside the R-matrix sphere the energy-independent wavefunction of scattering plus target electrons is represented by:

$$\Psi_k = \mathcal{A} \sum_i a_{i,k} \Phi_i(\boldsymbol{x}_1, \ldots, \boldsymbol{x}_N) F_{i,k}(\boldsymbol{x}_{N+1}) + \sum_j b_{j,k} \phi_j(\boldsymbol{x}_1, \ldots, \boldsymbol{x}_N, \boldsymbol{x}_{N+1}) \qquad (1)$$

where $\mathcal{A}$ is an anti-symmetrization operator and $N = 2$ for an H_2 target. The first term involves a sum over products of target states, Φ_i, and continuum orbitals $F_{i,k}$. With a

Table 2. Calculated ground state energy (in Hartree) and vertical excitation energies (in eV) for H_2 with internuclear separation of 1.4 a_0 compared with accurate theoretical estimates. For comparison the observed (non-vertical) excitation threshold are also given. The numbers in brackets are the number of full CI configurations used in our calculations.

State	This work	'Exact'	Experiment[a]
X $^1\Sigma_g^+$	−1.165801(28)	−1.1744744[b]	
b $^3\Sigma_u^+$	10.45(21)	10.62[b]	
a $^3\Sigma_g^+$	12.41(15)	12.54[c]	11.83
c $^3\Pi_u$	12.60(21)	12.73[d]	11.72
B $^1\Sigma_u^+$	13.15(21)	12.75[c]	11.19
E,F $^1\Sigma_g^+$	13.25(28)	13.14[e]	12.35
C $^1\Pi_u$	13.11(21)	13.23[f]	12.30

[a] Sharp (1971).
[b] Kolos and Wolniewicz (1965).
[c] Kolos and Wolniewicz (1968).
[d] Kolos and Rychlewski (1977).
[e] Interperlated from Kolos and Dressler (1985).
[f] Rothenberg and Davidson (1966).

CI target wavefunctions this term is generated by constructing the Hamiltonian matrix elements appropriate for each configuration of the appropriate target representation. These matrix elements are then contracted together using the coefficients of target configurations generated in the relevant target CI calculation.

The second term in (1) involves a sum over configurations where all electrons are placed in molecular orbitals belonging to the target. These configurations allow for high-l terms important in the region of the nuclear singularities, relaxation of the orthogonality condition described below and short-range target polarization effects. Because we have used a full CI representation of our H_2 target, all possible L^2 configurations were included in our expansion without risk of overcorrelating the continuum electron.

Continuum basis functions are expressed as a partial-wave expansion about the molecular centre of mass. The radial parts of these functions are generated numerically as solutions of suitable one-dimensional model problems and subject to boundary conditions on the R-matrix boundary which are relaxed by using a Buttle correction (Gillan *et al* 1987). In this work all solutions of the isotropic potential given by the ground-state SCF wavefunction lying below 5 Ryd were retained such that $l \leq 6$ and $m \leq 3$. The functions were transformed into an orthonormal set of molecular orbitals by Lagrange orthogonalizing (Tennyson *et al* 1987) the σ_g and π_u sets each to the two lowest target orbitals of the appropriate symmetry, and the σ_u and π_g sets each to the lowest target orbital. The resulting continuum orbitals are then Schmidt orthogonalized to the full set of target orbitals. The number of target orbitals used in the Lagrange orthogonalization was kept as low as possible and only increased if the calculations betrayed any sign of linear dependence—this typically manifests itself by the presence of one or more unphysically low R-matrix poles. Thus for example the six-state calculations in I required only one σ_g target orbital to be Lagrange orthogonalized, however the more diffuse 2s(σ_g) orbital ($\zeta = 0.6$ instead of 0.8) used in the present work caused linear dependence even in one-state calculations with this orthogonalization procedure.

The inner-region problem, defined by determining the variational coefficients in (1), was solved using a program suite adapted from the ALCHEMY quantum chemistry package (McLean 1971, Noble 1982). The only other exceptional feature of the present calculations is that the diffuse nature of several of the excited target states meant that we used a large, by molecular standards, R-matrix sphere of radius 20 a_0. This meant that care had to be taken with the evaluation of the long-range portions of the integrals for which we used double the default (Noble 1982) number of quadrature points.

Solutions from the inner region are used to construct R matrices on the boundary (Gillan *et al* 1987, Morgan 1990). These R matrices were then propagated (Morgan 1984a) to a radius of 100 a_0 and solutions to the scattering problem obtained by (Gailitis) asymptotic expansion techniques (Noble and Nesbet 1984). From these solutions K matrices, and hence eigenphase sums, and T matrices, and hence cross sections, were constructed. In these calculations all the diagonal and off-diagonal dipole and quadrupole moments (calculated as in Gillan *et al* (1990)) were retained in the outer-region potential expansion.

3. Results

Figures 1 to 5 present eigenphase sums as a function of collision energy for the lowest eight symmetries of the e^-–H_2 system. The curves represent 320 calculations at a grid of scattering energies separated by 0.01 eV, with small gaps near each threshold. Further calculations using a finer energy grid were performed to clarify any unresolved features and about seemingly discontinuous thresholds. These were sufficient to demonstrate that all the features in the figures are genuine and not caused by the smoothing of our plotting program or the indeterminacy of the eigenphases to modulo π.

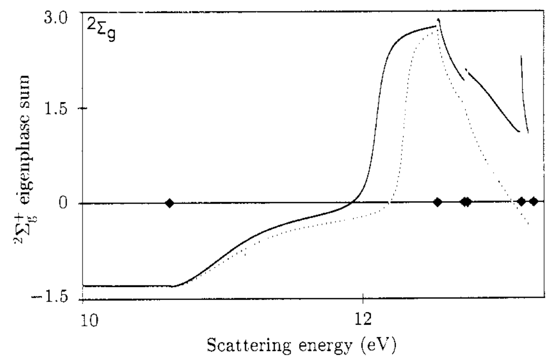

Figure 1. $^2\Sigma_g^+$ eigenphase sums for e^-–H_2 collisions as a function of scattering energy in eV. Full curve, seven-state model; dotted curve, six-state model of I.

The only area of uncertainty is on passing through the thresholds, which are marked on the zero line of the figures. In most cases the eigenphase sum was shown to be continuous through the thresholds—for example the $^2\Sigma_g^+$ symmetry eigenphase sums were found to continuous on passing through the b $^3\Sigma_u^+$ threshold despite the apparent glitch in figure 1. In some cases continuity was less obvious and there remains the possibility of very narrow, unresolved threshold features. In particular narrow

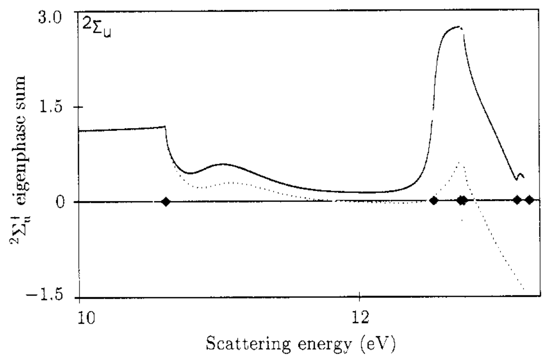

Figure 2. $^2\Sigma_u^+$ eigenphase sums for e^-–H_2 collisions as a function of scattering energy in eV. Full curve, seven-state model; dotted curve, six-state model of I.

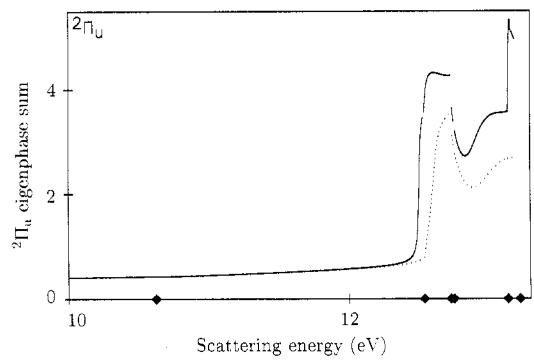

Figure 3. $^2\Pi_u$ eigenphase sums for e^-–H_2 collisions as a function of scattering energy in eV. Full curve, seven-state model; dotted curve, six-state model of I.

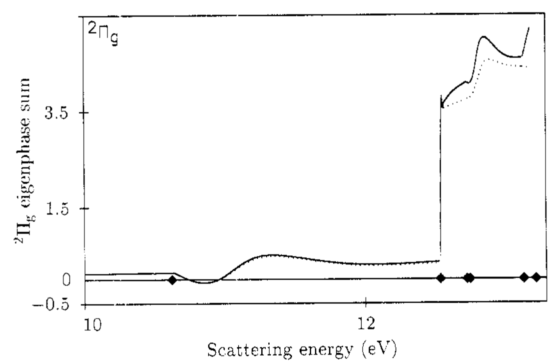

Figure 4. $^2\Pi_g$ eigenphase sums for e^-–H_2 collisions as a function of scattering energy in eV. Full curve, seven-state model; dotted curve, six-state model of I.

resonances with $^2\Pi_u$ and $^2\Pi_g$ symmetries were identified just above the E,F $^1\Sigma_g^+$ and a $^3\Sigma_g^+$ thresholds respectively. These resonances proved to be too close to the thresholds to be fitted. In only one case, the $^2\Sigma_g^+$ symmetry at the E,F $^1\Sigma_g^+$ threshold, see figure 1, is there a significant discontinuity which could not be accounted for by calculations whose nearest energy was 1×10^{-5} Ryd from the threshold. For comparison,

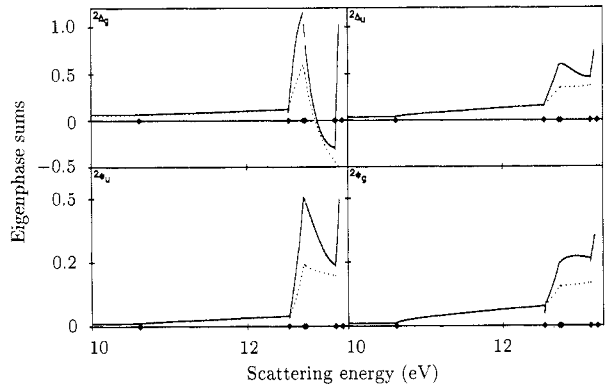

Figure 5. $^2\Delta_g$, $^2\Delta_u$, $^2\Phi_u$ and $^2\Phi_g$ eigenphase sums for e^-–H_2 collisions as a function of scattering energy in eV. Full curve, seven-state model; dotted curve, six-state model of I.

figures 1 to 5 also give the eigenphase sums computed using the six-state model of I; as one would expect the seven-state eigenphase sums are uniformly higher than those given by the six-state model.

Because of their great experimental importance, we have tabulated the resonances and other features in our eigenphase sums. Where possible we have attempted to fit these resonances to a Breit–Wigner form using an automatic detection and fitting procedure (Tennyson and Noble 1984). The results of these fits are given in table 3, which also give assignments to some of these features using the experimental classification scheme. In general rapid rises in the eigenphase sums of less than unity could not be fitted as resonances and are classified as features. Some, but not all, of these features would appear to be resonances truncated by a nearby threshold. We note that none of the features in the higher three symmetries of figure 5 are of large enough amplitude to be considered resonances.

Table 3. Resonance positions, E_{res}, and widths, Γ_{res}, for H_2^- with internuclear separation of 1.4 a_0 using a seven-state model.

Symmetry	E_{res} (eV)	Γ_{res} (eV)	Assignment
$^2\Sigma_g^+$	10.94	1.24	$1\sigma_g^1\ 1\sigma_u^2$
	12.10	0.106	'a' $1\sigma_g^1 2\pi_u^1 2\pi_u'^1$
$^2\Sigma_u^+$	10.91		'feature'
	12.54	0.073	'c'/'e' $1\sigma_g^1 2\pi_u^1 2\pi_g^1$
$^2\Pi_u$	12.50	0.018	'c'/'e' $1\sigma_g^1 2\pi_u^1 2\sigma_g^1$
	12.95	0.175	'feature'
$^2\Pi_g$	11.05	0.46	'feature'
	12.80	0.080	'd' $1\sigma_g^1 2\pi_u^1 2\sigma_u^1$?
$^2\Delta_g$	12.55	0.21	'resonance'
	13.16	0.058	'resonance'

Of course it is cross sections rather than eigenphase sums which are observed experimentally. Figures 6 to 11 present our total cross sections for electronic excitation from the ground X $^1\Sigma_g^+$ state to the six electronically excited states explicitly included in our seven-state calculations. These cross sections were obtained by summing the contributions for all the symmetries up to and including $^2\Phi_g$. Plotted for comparison are both experimental and previous theoretical results.

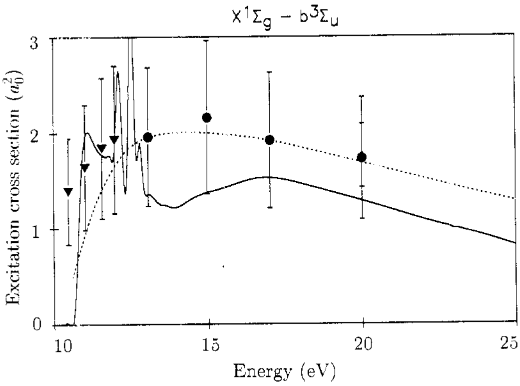

Figure 6. Total X $^1\Sigma_g^+$ → b $^3\Sigma_u^+$ excitation cross sections, in a_0^2, as a function of energy, in eV, for e^-–H_2 collisions. Theory: full curve, seven-state model (this work); broken curve, Baluja *et al* (1985). Experiment: ●, Nishimura and Danjo (1986); ▲, Khakoo *et al* (1987); ▼, Hall and Andric (1984).

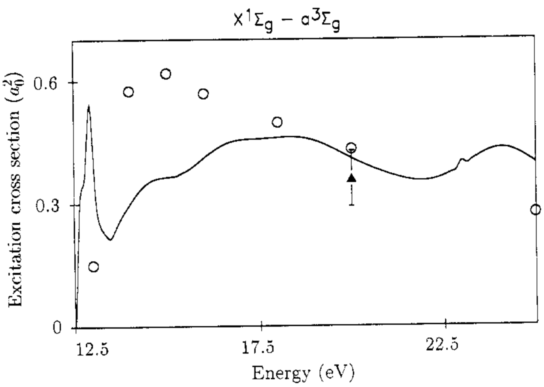

Figure 7. Total X $^1\Sigma_g^+$ → a $^3\Sigma_g^+$ excitation cross sections, in a_0^2, as a function of energy, in eV, for e^-–H_2 collisions. Theory: full curve, seven-state model (this work); ○, Lima *et al* (1988). Experiment: ▲, Khakoo and Trajmar (1986).

4. Discussion

Figures 1 and 5 are remarkable for the complexity of the structures displayed by the eigenphase sums. The *R*-matrix method is particularly well suited to mapping such complicated features as it is relatively cheap to repeat the energy-dependent portion of the calculations at a fine grid of energy points. To our knowledge no previous calculations on a molecular target have seen such richness of features, which

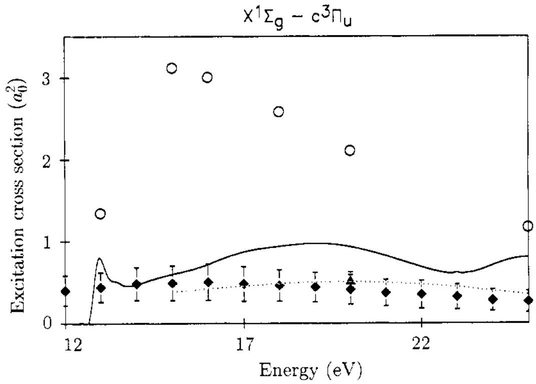

Figure 8. Total X $^1\Sigma_g^+ \rightarrow$ c $^3\Pi_u$ excitation cross sections, in a_0^2, as a function of energy, in eV, for e^-–H_2 collisions. Theory: full curve, seven-state model (this work); dotted curve, Lee *et al* (1982); ○, Lima *et al* (1988). Experiment: ♦, Mason and Newell (1986b); ▲, Khakoo and Trajmar (1986).

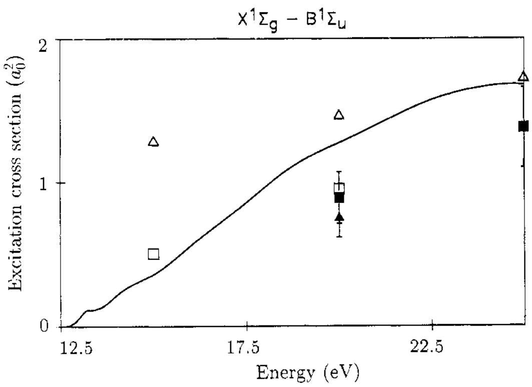

Figure 9. Total X $^1\Sigma_g^+ \rightarrow$ B $^1\Sigma_u^+$ excitation cross sections, in a_0^2, as a function of energy, in eV, for e^-–H_2 collisions. Theory: full curve, seven-state model (this work); □, Gibson *et al* (1987); △, Redmon *et al* (1985). Experiment: ■, Ajello *et al* (1984); ▲, Khakoo and Trajmar (1986).

have, however, been found in some atomic collision calculations (e.g. Clark and Taylor 1982). This is a manifestation of the sophistication of these calculations compared with previous studies on molecular systems.

Comparison of the six-state and seven-state eigenphase sums shows that below about 12 eV our results are stable to including the extra state whereas at higher energies they show a strong sensitivity to the model used. A recent study of the second ('a', see table 3) $^2\Sigma_g^+$ resonance (da Silva *et al* 1990) suggests that this resonance is particularly sensitive to the inclusion of the (closed) E,F $^1\Sigma_g^+$ state. However, while we believe our results below 12 eV are well converged with respect to the coupled-state expansion, it is not possible for us to rule out sensitivity of the eigenphases to the inclusion of other, higher-lying, closed states in the calculation.

This enhanced sensitivity of the eigenphase sums would appear to be caused by the presence of a number of overlapping resonances and resonance-like features. Small changes in the positions and widths of these resonances have a disproportionately

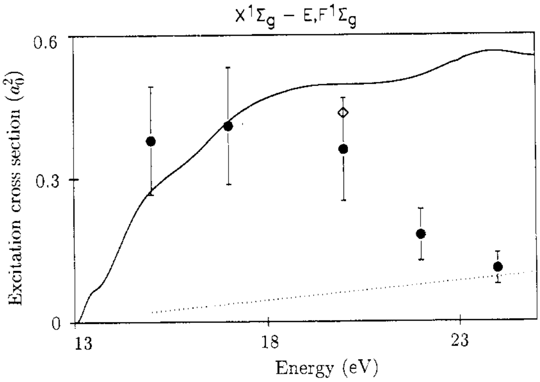

Figure 10. Total X $^1\Sigma_g^+ \rightarrow$ E,F $^1\Sigma_g^+$ excitation cross sections, in a_0^2, as a function of energy, in eV, for e^-–H_2 collisions. Theory: full curve, seven-state model (this work); dotted curve, Lee *et al* (1982); ◇, Arrighini *et al* (1980). Experiment: ●, *lower limit* of Watson and Anderson (1977).

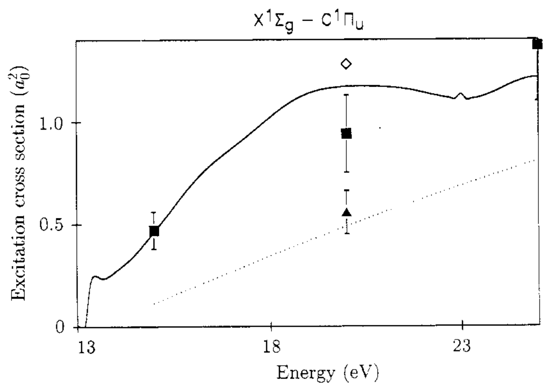

Figure 11. Total X $^1\Sigma_g^+ \rightarrow$ C $^1\Pi_u$ excitation cross sections, in a_0^2, as a function of energy, in eV, for e^-–H_2 collisions. Theory: full curve, seven-state model (this work); dotted curve, Lee *et al* (1982); ◇, Arrighini *et al* (1980). Experiment: ■, Ajello *et al* (1984); ▲, Khakoo and Trajmar (1986).

large effect on the eigenphase sums because of interference effects. For example in the $^2\Sigma_u^+$ symmetry calculations (see figure 2), a small 'feature' associated with the c $^3\Pi_u$ threshold in the six-state calculations of I is resolved as full resonance straddling the a $^3\Sigma_g^+$ threshold in the present seven-state calculations.

There have been no previous scattering calculations comparable with the present study (and that in I), therefore many of the 'features' shown in figures 1 to 5, the most important of which are listed in table 3, have not been previously noted. Comparable theoretical studies have been performed using L^2 techniques, the results of which are summarized in table 4. The most comprehensive calculations at $R = 1.4a_0$ are due to Buckley and Bottcher (1977) whose predictions are in good agreement with ours. In their work they assigned both their $^2\Sigma_u^+$ resonance at 12.41 eV and their $^2\Pi_u$ resonance at 12.70 to the 'c' series.

The work of DeRosa *et al* (1988) only provides an upper limit on the resonance position as these workers give the absolute value of the H_2^- energy, but fail to give

Table 4. Comparison of theoretical predictions of resonance positions, in eV, for H_2^- with internuclear separation of 1.4 a_0.

Symmetry	Label	ETW[a]	BB[b]	DGSS[c]	I[d]	This work
$^2\Sigma_g^+$	$1\sigma_g^1\ 1\sigma_u^2$	10.68	10.94		10.96[e]	10.94
$^2\Sigma_g^+$	'a'	12.32	12.16		12.30	12.10
$^2\Sigma_u^+$	'c'/'e'		12.41	≤ 12.31	NO[f]	12.54
$^2\Pi_u$	'c'/'e'		12.70		12.60	12.50

[a] Elizer *et al* (1967).
[b] Buckley and Bottcher (1977).
[c] DeRosa *et al* (1988).
[d] Brandhett and Tennyson (1990).
[e] Misprinted in I.
[f] Not observed.

a comparable value for the ground state of H_2 in their model. DeRosa *et al*, unlike the other L^2 calculations mentioned, estimate resonance widths. However their estimate of 0.67 eV for the width of 'c'/'e' $^2\Sigma_u^+$ resonance would appear much too large; furthermore these authors predict this resonance to be the *third* of $^2\Sigma_u^+$ symmetry in contrast to all other work, including this, which finds only one lower-lying resonance of $^2\Sigma_u^+$ symmetry.

Unsurprisingly, the resonance positions (and widths) of the present calculations are in good agreement with those obtained in I. Adding the extra state lowers all the resonance positions slightly and the 'a' $^2\Sigma_g^+$ resonance by 0.2 eV. More unusually, as can be seen from figure 1, this resonance is actually *broader* in the seven-state calculation.

There are considerable experimental data on the resonances associated with the electronic thresholds studied. The resonances studied are sufficiently narrow to support significant vibrational structure giving resonance series. To make comparison with these observed series, labelled 'a' to 'g' (Schulz 1973), it is necessary to allow for the fact we have only considered vertical excitation at a single frozen geometry. Most of these resonances have been associated with a particular 'parent' state. In fact the resonances denoted 'a', 'c', 'd' and 'e' are all thought to be associated with the c $^3\Pi_u$ state (Schulz 1973). In table 3 the molecular orbital designations of these states are based upon this assignment. If this parent state is known, the association can be made by shifting our resonance position by the difference between the vertical excitation energy and the adiabatic excitation energy of the parent state.

Schulz (1973) attributes the 'a' and 'c' series to $^2\Sigma_g^+$ and $^2\Pi_u$ symmetries respectively, with c $^3\Pi_u$ as the parent state. Allowing for the shifts places our second $^2\Sigma_g^+$ and first $^2\Pi_u$ resonances are at 11.09 and 11.49 eV respectively. Experimentally the 'a' and 'c' series have been observed with origins in the range 11.28–11.34 eV and 11.43–11.50 (Schulz 1973, Mason and Newell 1986a). However the seven-state calculations, in contrast to the six-state calculations of I, also have a resonance of $^2\Sigma_u^+$ symmetry in this energy region. This occurs with a shifted energy of 11.53 eV.

Experimental estimates for the widths of these resonances are limited. Joyez *et al* (1973) put an upper limit on the widths of the 'a' and 'c' series in H_2 of 0.016 eV. This is smaller than the widths of our resonances at the appropriate energies, except for the ones with $^2\Pi_u$ symmetry, which are nearer the earlier estimate of 0.08 eV (Weingartshofer *et al* 1970). However, Joyez *et al* found the width to be isotope dependent, obtaining a value of 0.03 eV for their D_2 experiments (Schulz 1973). If this observation is correct, and other experiments show markedly different behaviour between H_2 and D_2 (e.g. Bose and Linder 1979), then the widths of the resonances would appear to depend on factors that are beyond the scope of a fixed-nuclei calculation.

The 'd' and 'e' series have the same energy spacings as the 'a' and 'c' series respectively, but different overall symmetry. These series were proposed to explain unusual observed angular distributions. Our discovery of nearby resonances with $^2\Sigma_u^+$ and $^2\Pi_u$ total symmetry, close in energy to the 'c' and 'e' series lends some support to this interpretation. We also note that we obtain a suitably narrow, but truncated, resonance feature at 12.80 eV with $^2\Pi_g$ symmetry. This is the symmetry proposed by Weingartshofer *et al* (1970) for the 'd' series. However, we remain cautious about matching these features with the experimental observations. Initial studies of the differential cross sections near these resonances suggests that the angular distribution is sensitive to which channel is being used for the observation. We are currently undertaking a full study of the differential cross sections in the 10–15 eV resonance region (Branchett *et al* 1990).

Figures 6 to 11 compare our electronic excitation cross sections with previous theoretical estimates and experimental observations. It is not possible, and probably not desirable, to include all the previous data on these figures. We have therefore selected the most recent and reliable results for comparison. Our results are generally in good agreement with the available experimental estimates. The agreement with previous, less accurate, theoretical calculations is more patchy.

Figures 6 to 11 do not give results for the six-state calculations of I because, despite the sensitivity of the eigenphase sums to the model used, the magnitude of the excitation cross sections were not greatly different from those calculated here. We note, particularly in figures 7 and 9, that the experimental results appear to have a lower threshold than our 'exact' one. This is an artefact of our use of a fixed H_2 bond length. As all the excited states are either repulsive or have minima at internuclear separations larger than 1.4 a_0, excitation from the longer H_2 internuclear separations sampled by the motion of the vibrational ground state has a lower threshold.

Whereas our calculations show a number of features due to the resonances detailed in table 3, none of the previous results show these features—see in particular figures 6 and 7. This is because the previous theoretical models, which excluded practically all multichannel effects, did not allow for Feshbach resonances; while the experimental results are either too inaccurate or at too coarse an energy grid to resolve narrow features due to resonances. So for example, although our X $^1\Sigma_g^+ \rightarrow$ b $^3\Sigma_u^+$ excitation cross sections, figure 6, display a markedly different energy dependence to the previous two-state R-matrix results of Baluja *et al* (1985) (whose cross sections are similar to those of Schneider and Collins (1985) and Lima *et al* (1985)), the experimental results are not sufficiently accurate to distinguish between the different calculations.

This is even more true for the X $^1\Sigma_g^+ \rightarrow$ a $^3\Sigma_g^+$ excitation cross sections, figure 7, where the single experimental point agrees well with the two theories which in turn disagree at all other energies. We note that the calculation of Lima *et al* (1988) shows a slowly rising broad peak in the excitation cross section above threshold in contrast to our prediction of a sharp threshold spike. This difference seems to be typical between calculations that include and neglect multichannel effects.

For the X $^1\Sigma_g^+ \rightarrow$ c $^3\Pi_u$ excitation cross sections, figure 8, neglect of multichannel effects appears to lead to a significant overestimate of the cross section by Lima *et al* (1988). Subsequent tests by Lee *et al* (1990) have shown that the use of correlated target wavefunctions alone is not sufficient to overcome this discrepancy. For this excitation the distorted-wave calculations of Lee *et al* (1982) give very good agreement with experiment. It should be noted that the same calculations give poor agreement for other electronic excitations, see figures 10 and 11.

The cross sections for excitation to singlet excited states display rather different behaviour from the triplet excitations discussed above. The cross sections are smaller and show less structure with only gradual increases from threshold. This behaviour is particularly marked for the dipole-allowed X $^1\Sigma_g^+ \rightarrow$ B $^1\Sigma_u^+$ excitation cross sections, figure 9. In this case our results are in good agreement with the calculations of Gibson *et al* (1987). We note however that the distorted-wave calculations of Fliflet and McKoy (1980) appear to greatly overestimate the excitation cross section and were generally too big to include on the figure. The calculations of Redmon *et al* (1985) used an impact-parameter method which neglects exchange and, as shown by the figure, gives better results at higher energies.

There is little previous work on the X $^1\Sigma_g^+ \rightarrow$ E,F $^1\Sigma_g^+$ excitation cross sections, figure 10. Our results are in surprisingly good agreement with *lower estimates* obtained experimentally by Watson and Anderson (1977) and agree well with the Born–Ochkur calculation of Arrighini *et al* (1980). We note that Arrighini *et al* used extended CI targets in their calculation.

Our results for the X $^1\Sigma_g^+ \rightarrow$ C $^1\Pi_u$ excitation cross sections, figure 11, appear in good agreement with the renormalized (Ajello *et al* 1984) observations of Ajello *et al* (1982) and the Born–Ochkur calculations of Arrighini *et al* (1980). Conversely the lower experimental value of Khakoo and Trajmar at 20 eV is in better agreement with the distorted-wave calculations of Lee *et al* (1982).

Several of our cross sections show structure at energies above 15 eV; in particular there appears to be a resonance at 23 eV. Pseudo-resonances are an expected artefact of our calculations in energy regions where open channels have been neglected and we therefore would treat any features in this energy region with caution. Furthermore, simple flux arguments suggest that our calculations would overestimate cross sections in the energy region where open electronic states have been omitted from the model. This behaviour is demonstrated in the comparison of two- and seven-state calculations in figure 6.

5. Conclusions

We have presented results for electron–H_2 collisions using seven coupled electronic states of H_2 represented by accurate, correlated wavefunctions. The calculations have generated a wealth of data on cross sections and resonance parameters, most of it in good agreement with experiment. These calculations represent a very significant advance on previous studies on this fundamental problem. It is our plan to extend this work by detailed consideration of the differential cross sections both for resonant and non-resonant collisions in the 10–20 eV scattering region (Branchett *et al* 1990). Such calculations are important because it is only via differential cross sections that the observed angular distributions of the many resonance series in this region may be understood, and because the available experimental data for non-resonant electronic excitation are very much more accurate for differential rather than total cross sections.

Acknowledgments

We thank Nigel Mason for helpful discussions during the course of this work. This work was supported by Science and Engineering Research Council grant GR/F/14550.

References

Ajello J M, Srivastava S K and Yung Y L 1982 *Phys. Rev.* A **25** 2485–98
Ajello J M, Shemansky D, Kwok T L and Yung Y L 1984 *Phys. Rev.* A **29** 636–53
Arrighini G P, Biondi F and Guidotti C 1980 *Mol. Phys.* **41** 1501–14
Baluja K L, Noble C J and Tennyson J 1985 *J. Phys. B: At. Mol. Phys.* **18** L851–5
Bardsley J N and Cohen J S 1978 *J. Phys. B: At. Mol. Phys.* **11** 3645–54
Bose N and Linder F 1979 *J. Phys. B: At. Mol. Phys.* **12** 3805–17
Branchett S E and Tennyson J 1990 *Phys. Rev. Lett.* **64** 2889–92
Branchett S E, Tennyson J and Morgan L A 1990 *J. Phys. B: At. Mol. Opt. Phys.* to be submitted
Buckley B D and Bottcher C 1977 *J. Phys. B: At. Mol. Phys.* **10** L635–40
Clark C W and Taylor K T 1982 *J. Phys. B: At. Mol. Phys.* **18** L213–9
da Silva A R J, Lima M A P, Brescansin L M and McKoy V 1990 *Phys. Rev.* A **41** 2903–5
Danby G and Tennyson J 1990 *J. Phys. B: At. Mol. Opt. Phys.* **23** 1005–16
DeRosa E F, Gislason E A, Sabelli N H and Sluis K M 1988 *J. Chem. Phys.* **88** 4878–83
Elizer I, Taylor H S and William J K 1967 *J. Chem. Phys.* **47** 2165–77
Fliflet A W and McKoy V 1980 *Phys. Rev.* A **21** 1863–75
Fraga S and Ransil B 1961 *J. Chem. Phys.* **35** 1967–77
Gibson T L, Lima M A P, McKoy V and Huo W M 1987 *Phys. Rev.* A **35** 2473–8
Gillan C J, Nagy O, Burke P G, Morgan L A and Noble C J 1987 *J. Phys. B: At. Mol. Phys.* **20** 4585–603
Gillan C J, Noble C J and Burke P G 1988 *J. Phys. B: At. Mol. Opt. Phys.* **21** L53–9
—— 1990 *J. Phys. B: At. Mol. Opt. Phys.* **23** L407–13
Hall R I and Andric L 1984 *J. Phys. B: At. Mol. Phys.* **17** 3815–25
Joyez G, Comer J and Read F H 1973 *J. Phys. B: At. Mol. Phys.* **6** 2427–40
Khakoo M A and Trajmar S 1986 *Phys. Rev.* A **34** 146–56
Khakoo M A, Trajmar S, McAdams R and Shyn T W 1987 *Phys. Rev.* A **35** 2832–7
Kolos W and Dressler K 1985 *J. Chem. Phys.* **82** 3292–9
Kolos W and Rychlewski J 1977 *J. Mol. Spectrosc.* **66** 428–40
Kolos W and Wolniewicz L 1965 *J. Chem. Phys.* **43** 2429–41
—— 1968 *J. Chem. Phys.* **48** 3672–80
Lee M-T, Luchesse R R and McKoy V 1982 *Phys. Rev.* A **26** 3240–8
Lee M-T, Machado L E, Leal E P, Brescansin L M, Lima M A P and Machado F B C 1990 *J. Phys. B: At. Mol. Opt. Phys.* **23** L233–7
Lima M A P, Gibson T L, Takatsuka K and McKoy V 1985 *J. Phys. B: At. Mol. Phys.* **18** L865–70
Lima M A P, Gibson T L, McKoy V and Huo W M 1988 *Phys. Rev.* A **38** 4527–36
McConkey J W, Trajmar S and King G C M 1988 *Comment. At. Mol. Phys.* **22** 17–49
Mason N J and Newell W R 1986a *J. Phys. B: At. Mol. Phys.* **18** L203–7
—— 1986b *J. Phys. B: At. Mol. Phys.* **19** L587–91
McClean A D 1971 *Conf. Potential Energy Surfaces in Chemistry* ed W A Lester Jr (San Jose: IBM Research Laboratory) p 87
Morgan L A 1984a *Comput. Phys. Commun.* **31** 419–22
—— 1984b *J. Phys. B: At. Mol. Phys.* **19** L439–45
—— 1990 *Proc. 16th Int. Conf. on Physics of Electronic and Atomic Collisions* ed A Dalgarno *et al* (Plenum: New York) Invited Papers and Progress Reports pp 96–102
Morgan L A and Burke P G 1988 *J. Phys. B: At. Mol. Opt. Phys.* **21** 2091–105
Morgan L A, Burke P G and Gillan C J 1990 *J. Phys. B: At. Mol. Opt. Phys.* **23** 99–103
Nesbet R K, Noble C J and Morgan L A 1986 *Phys. Rev.* A **34** 2798–808
Nishimura N and Danjo A 1986 *J. Phys. Soc. Japan* **55** 3031–6
Noble C J 1982 *Daresbury Laboratory Technical Memorandum* DL/SCI/TMT33T
Noble C J and Nesbet R K 1984 *Comput. Phys. Commun.* **33** 399–411

Noble C J and Burke P G 1986 *J. Phys. B: At. Mol. Phys.* **19** L35–9
Pasquerault D, Defrance A and Hagene M 1985 *J. Phys. B: At. Mol. Phys.* **18** L871–3
Redmon M J, Garrett B C, Redmon L T and McCurdy 1985 *Phys. Rev.* A **32** 3354–65
Rescigno T N and Schneider B I 1988 *J. Phys. B: At. Mol. Opt. Phys.* **21** L691–5
Rothenberg S and Davidson E R 1966 *J. Chem. Phys.* **44** 730–7
Schneider B I and Collins L A 1985 *J. Phys. B: At. Mol. Phys.* **18** L857–63
Schulz G J 1973 *Rev. Mod. Phys.* **45** 423–86
Sharp T E 1971 *At. Data* **2** 119–69
Shemansky D E, Ajello J M and Hall D T 1985 *Astrophys. J.* **296** 765–73
Spence D 1974 *J. Phys. B: At. Mol. Phys.* **7** L87–90
Tawara H and Phaneuf R A 1988 *Comment. At. Mol. Phys.* **21** 177–93
Tawara H, Itikawa Y, Nishimura N and Yoshimo M 1990 *J. Phys. Chem. Ref. Data* **19** 617–36
Tennyson J 1986 *J. Phys. B: At. Mol. Phys.* **19** 4255–63
—— 1988 *J. Phys. B: At. Mol. Opt. Phys.* **21** 805–16
Tennyson J and Noble C J 1984 *Comput. Phys. Commun.* **32** 421–4
—— 1985 *J. Phys. B: At. Mol. Phys.* **18** 155–65
—— 1986 *J. Phys. B: At. Mol. Phys.* **19** 4025–33
Tennyson J, Noble C J and Salvini S 1984 *J. Phys. B: At. Mol. Phys.* **17** 905–12
Tennyson J, Burke P G and Berrington K A 1987 *Comput. Phys. Commun.* **47** 207–16
Watson J Jr and Anderson R J 1977 *J. Chem. Phys.* **66** 4025–30
Weingartshofer A, Ehrhardt H, Hermann V and Linder F 1970 *Phys. Rev.* A **2** 294–304
Weingartshofer A, Clarke E M, Holmes J K and McGowan J W 1975 *J. Phys. B: At. Mol. Phys.* **8** 1552–69